

Synthesis of a smart bisbenzoxazine with combined advantages of bismaleimide and benzoxazine resins and its unexpected formation of very high performance cross-linked polybenzoxazole

Kan Zhang^{a,*}, Boran Hao^a, Hatsuo Ishida^{b,**}

^a School of Materials Science and Engineering, Jiangsu University, Zhenjiang, 212013, China

^b Department of Macromolecular Science and Engineering, Case Western Reserve University, Cleveland, OH, 44106, USA

ARTICLE INFO

Keywords:

Benzoxazine
Bismaleimide
Polybenzoxazine
High-performance

ABSTRACT

We report a bisbenzoxazine thermosetting system, oHPMI-ddm, which shows combined advantages of both bismaleimide and benzoxazine resins. The chemical structure of oHPMI-ddm has been identified by FT-IR and NMR spectroscopies, and its polymerization processes have been investigated using differential scanning calorimetry (DSC) and *in situ* FT-IR. The resulting polybenzoxazine derived from this thermosetting system exhibits significantly higher thermal stability than thermosets polymerized from the commercialized 4,4'-diaminodiphenylmethane based bisbenzoxazine (PH-ddm) and bismaleimide (DDM-BMI). This newly obtained benzoxazine also shows a unique structural thermal rearrangement in comparison to the cross-linked polybenzoxazole in a similar manner as other reported smart *ortho*-benzoxazines, although it has no obvious hydrogen bond forming group and cannot form 5- or 6-membered intramolecular interaction. Such conversion from polybenzoxazine to polybenzoxazole has been confirmed by both *in situ* FT-IR and solid state ¹³C NMR. Furthermore, the finally obtained cross-linked polybenzoxazole possesses outstanding properties of high thermal stability, excellent flame retardancy and low dielectric constant, indicating great potential for high performance material applications.

1. Introduction

Bismaleimide (BMI) resins are a family of high-performance polymers that are generally used as matrix materials for industrial applications [1] [2] [3]. BMI polymers [3,4] have many attractive properties, such as resistance to high-temperature, radiation, and chemical degradation as well as good mechanical performance [1]. However, traditional unmodified BMI resins possess some shortcomings, including poor solubility in common organic solvents and high melting temperature due to its rigid and symmetrical structure. These undesirable properties cause difficulties in the processing of resins. In addition, the polymerized BMI resins exhibit high brittleness because of their highly cross-linked networks with rigid molecular backbones [5,6]. The above shortcomings in BMI resins have evidently restricted exploration of their further applications. In order to improve the ductility of BMI resins, researchers have developed various approaches, including blending them with elastomers [7] and thermoplastics [8], or

copolymerizing them with allyl [9], cyanate [10], amine [11] and benzoxazine-related compounds [12,13].

Polybenzoxazine thermosets have attracted increasing attentions in recent years because they exhibit many outstanding properties [14–18], such as near-zero shrinkage upon polymerization [19], outstanding thermal [20,21] and mechanical properties [22–25], low surface energy [24,25] and excellent electric properties [26]. The most unique character of polybenzoxazine thermosets is the high molecular design flexibility of their precursor, namely benzoxazines, which enables synthesis of various cross-linked networks to tailor the target performance [14, 15]. Specifically, addition of smart functionalities from other high-performance polymers in benzoxazine resins provides a useful means to further improve already well-balanced, unique properties of polybenzoxazine thermosets.

Cross-linked polybenzoxazole (cPBO) thermosets with excellent mechanical and physical properties have been developed *via ortho*-amide or *ortho*-imide functionalized benzoxazine resins (Scheme 1)

* Corresponding author.

** Corresponding author.

E-mail addresses: zhangkan@ujs.edu.cn (K. Zhang), hxi3@cwru.edu (H. Ishida).

[27–30]. In general, the conventional method to obtain polybenzoxazoles is through the use of strong acids, which can dissolve both reaction intermediates and products [31,32]. However, using strong acids as reaction solvent is environmentally unfriendly, and such manufacturing approaches are unacceptable in most industries. In addition, difficulty of eliminating the residual solvent can lead to an aging problem at elevated temperature and humid environment via hydrolysis of benzoxazole ring. Thus, approaches for achieving cross-linked polybenzoxazoles (cPBOs) based on *ortho*-benzoxazines show many alternative advantages, such as excellent molecular design flexibility, requiring no strong acids, easy processability and cost efficiency. In our recent work, we synthesized a series of *ortho*-maleimide mono-benzoxazines, which expanded the family of known smart *ortho*-benzoxazine [33]. Unfortunately, the thermal conversion of *ortho*-hydroxylmaleimide into benzoxazoles was not evaluated in that study.

Due to the success of the above findings, we were encouraged to design a new thermosetting system, *o*HPMI-ddm, which presents structural features of both bisbenzoxazine and bismaleimide (Scheme 2). Previously, we developed a series of smart benzoxazines as cPBO precursors by designing monomers with an intramolecular 5- or 6-membered hydrogen bond group that is in the vicinity of the oxazine ring [27–30]. However, in this paper we report the first cross-linked polybenzoxazole based on *ortho*-maleimide benzoxazine. This newly obtained benzoxazine monomer has no obvious hydrogen bond forming group and cannot form 5- or 6-membered intramolecular interaction. This observation was totally unexpected. In addition, the conversion through neighboring hydroxyl and maleimide has never been evaluated. The detailed synthetic strategy, the thermally activated structural transformation, and the properties of the resulting thermosets will be discussed in the current work.

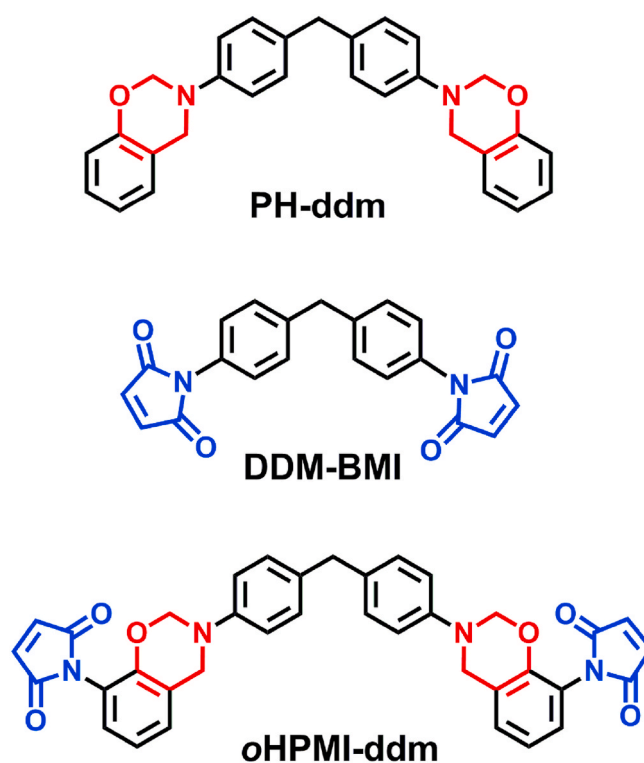
2. Experimental

2.1. Materials

p-Toluenesulfonic acid (*p*-TSA) (98%), maleic anhydride (98%), 2-aminophenol (>98%) and 4,4'-bismaleimidodiphenylmethane (DDM-BMI) were purchased from Aladdin Reagent, China, and used without further purification. 4,4'-Diaminodiphenylmethane (98%), paraformaldehyde (99%), aniline, toluene, isopropanol, dimethylformamide (DMF), sodium hydroxide (NaOH) and acetone were purchased from Energy Reagent, China. 1-(2-Hydroxyphenyl)-1*H*-pyrrole-2,5-dione (*o*HPMI) was synthesized according to the procedures reported by our group [33].

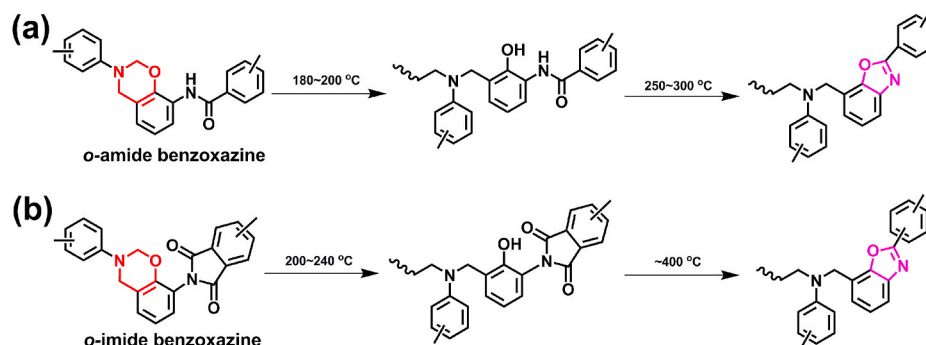
2.2. Characterization

All NMR spectra of benzoxazine samples, including ^1H and ^{13}C NMR, and 2 dimensional (2-D) ^1H - ^{13}C HMQC were recorded on a 400 MHz



Scheme 2. Chemical Structures of PH-ddm, DDM-BMI and *o*HPMI-ddm.

NMR spectrometer (Bruker AVANCE II). The average number of transients, 64 was used for proton NMR measurement, and 1024 was applied for carbon NMR testing. Fourier-transform infrared (FT-IR) spectra were recorded on a Nicolet Nexus 670 spectrometer, at a spectral resolution of 4 cm^{-1} (from 4000 to 400 cm^{-1}) using 64 co-added scans per spectrum. The spectrometer was equipped with a dry-air purging unit and deuterated triglycine detector. The benzoxazine sample was ground and pressed into a KBr pellet which was examined by the transmission method. Elemental analysis for the newly synthesized benzoxazines was carried out on an Elementar Vario EL-III analyzer. Thermograms of differential scanning calorimeter (DSC) were recorded on a NETZSCH DSC (Model 204f1) at different heating rates with a nitrogen flow rate of 60 mL/min . Dynamic mechanical analysis (DMA) was performed by a DMA analyzer (NETZSCH DMA/242E). A tension mode with an amplitude of $10\text{ }\mu\text{m}$ at a frequency of 1 Hz was used during the DMA testing, and the heating rate for DMA measurement was set as $3\text{ }^\circ\text{C/min}$. Thermogravimetric analyses (TGA) were performed on a NETZSCH STA449-C thermal analyzer at a heating rate of $10\text{ }^\circ\text{C/min}$. The dielectric constants (k) and dielectric loss ($\tan\delta$) of thermoset films were measured by the capacitance method at a frequency range from 100 Hz to 1 MHz



Scheme 1. Preparation of Cross-Linked Polybenzoxazoles via Thermal Conversion from *Ortho*-Amide (a) and *Ortho*-Imide (b) Functional Benzoxazines.

using a TZDM-RT-300 Dielectric Testing System Analyzer at room temperature. Silver paste was coated onto both surfaces of thermoset films before testing. The heat release rate (HRR, W/g) was recorded on a microscale combustion calorimeter (MCC, Fire Testing Technology) at a heating rate of 1 K/s from 100 to 750 °C. A stream of N₂ (flow rate of 80 mL/min) was mixed with a stream of O₂ (flow rate of 20 mL/min) before entering the combustion furnace (900 °C).

2.3. Methods

Synthesis of bis(4-(2H-benzo[e][1,3]oxazin-3(4H)-yl)phenyl)methane (abbreviated as PH-ddm). 4,4'-Diaminodiphenylmethane (1.98 g, 0.01 mol), phenol (1.88 g, 0.02 mol), paraformaldehyde (1.32 g, 0.044 mol) and 30 mL of toluene were added into a 100 mL single-neck flask. The mixture was magnetically stirred and then heated to reflux for 12 h. Afterwards, the crude product was washed with 1 N NaOH aqueous solution and distilled water 3 times on each step, and the product was then concentrated by a rotary evaporator. Further purification of the washed product was achieved by recrystallization in a 1:1 mixture of acetone and toluene to generate a white crystalline needle-like product. Next, the product was dried under vacuum at 50 °C for 48 h (yield ca. 75%). mp: 125 °C. ¹H NMR (400 MHz, CDCl₃), ppm: δ = 7.15–6.80 (16H, Ar), 5.35 (s, 4H, Ar-O-CH₂-NR, oxazine), 4.61 (s, 4H, Ar-CH₂-NR, oxazine), 3.83 (s, 2H, Ar-CH₂-Ar). FT-IR spectra (KBr), cm⁻¹: 1226 (C-O-C asymmetric stretching), 946 (oxazine ring related mode). Anal. calcd for C₂₉H₂₆N₂O₂: C, 80.16%; H, 6.03%; N, 6.45%. Found: C, 80.07%; H, 6.05%; N, 6.42%.

Synthesis of 1,1'-(3,3'-(4,4'-methylenebis(4,1-phenylene))bis(3,4-dihydro-2H-benzo[e][1,3]oxazine-8,3-diyl))bis(1H-pyrrole-2,5-dione) (abbreviated as oHPMI-ddm). 4,4'-Diaminodiphenylmethane (1.98 g, 0.01 mol), oHPMI (3.78 g, 0.02 mol), paraformaldehyde (1.32 g, 0.044 mol) and toluene (80 mL) were added into a 250 mL single-neck flask. The reaction mixture was stirred and heated to reflux for 24 h. Afterwards the solution was washed with distilled water for 3 times, and then the product sample was concentrated by a rotary evaporator. The washed product was further purified by recrystallization in a 1:1 of acetone-toluene to produce a light yellow crystalline product, which was then dried in a vacuum oven at 60 °C for 48 h (yield ca. 89%). mp: 105 °C. ¹H NMR (400 MHz, CDCl₃), ppm: δ = 7.08–6.93 (14H, Ar), 6.86 (s, 4H, -CH=CH-, maleimide), 5.31 (s, 4H, Ar-O-CH₂-NR, oxazine), 4.62 (s, 4H, Ar-CH₂-NR, oxazine), 3.82 (s, 2H, Ar-CH₂-Ar). FT-IR spectra (KBr), cm⁻¹: 1776 (C=O asymmetrical stretching) 1709 (C=O symmetrical stretching), 1229 (C-O-C asymmetric stretching), 920 (oxazine ring related mode), 836 (C-H wagging), 692 (out-of-plane of =C-H). Anal. calcd for C₃₇H₂₈N₄O₆: C, 71.14%; H, 4.52%; N, 8.97%. Found: C, 71.06%; H, 4.55%; N, 8.91%.

Preparation of Thermosets Based on PH-ddm, DDM-BMI and oHPMI-ddm. Polymerization of PH-ddm, DDM-BMI and oHPMI-ddm was performed by heating at 140, 160, 180, 200, 220 and 240 °C for 1 h at each step, to obtain poly(PH-ddm), poly(DDM-BMI) and poly(oHPMI-ddm), respectively.

ddm), respectively. Poly(oHPMI-ddm) was further treated at 300, 350 and 400 °C for 1 h at each step to obtain cPBO-oHPMI-ddm.

3. Results and discussion

3.1. Synthesis and characterization of benzoxazine monomers

In the current work, the pathway for preparing cPBO started from *ortho*-maleimide functionalized phenol (oHPMI) for synthesis of benzoxazine, then polymerizing and further structurally transforming to obtain cPBO-oHPMI-ddm. The bisbenzoxazine monomer with *ortho*-maleimide functionality, (oHPMI-ddm), was successfully synthesized using a primary amine, (4,4'-diaminodiphenylmethane), and paraformaldehyde as shown in Scheme 3. In addition, a counterpart benzoxazine without the maleimide group, PH-ddm, was prepared and highly purified.

The structures of benzoxazine monomers were identified by ¹H NMR, ¹³C NMR, and FT-IR analyses. Fig. 1 shows the ¹H NMR spectra of PH-ddm and oHPMI-ddm. The characteristic resonances assigned to the benzoxazine moiety, Ar-CH₂-N- and -O-CH₂-N- for PH-ddm are found at 4.61 and 5.35 ppm, respectively. These signals for oHPMI-ddm are located at 4.62 and 5.31 ppm, respectively. Besides the typical resonances attributed to Ar-CH₂-Ar in diaminodiphenylmethane are located at 3.83 and 3.82 ppm for PH-ddm and oHPMI-ddm, respectively. The ¹H NMR spectrum of oHPMI-ddm also confirms the maleimide functionality as observed by the presence of the protons of -CH=CH- at 6.86 ppm.

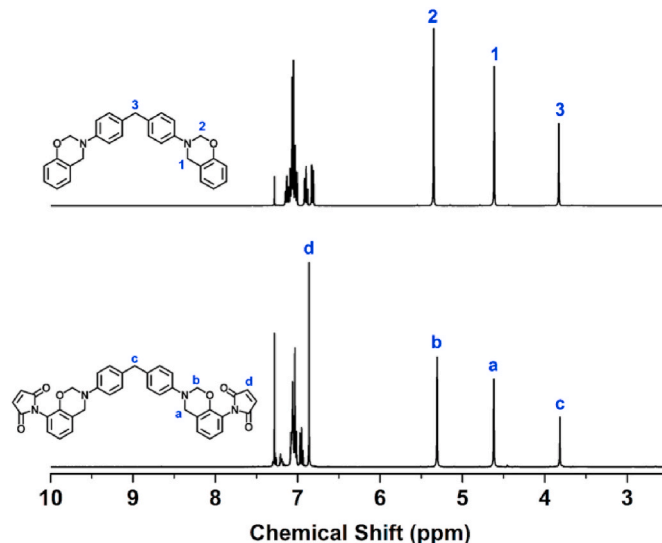
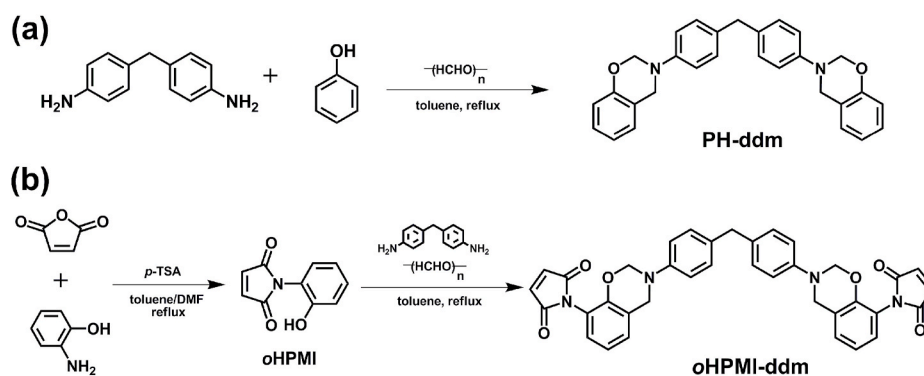


Fig. 1. ¹H NMR spectra of PH-ddm and oHPMI-ddm in CDCl₃.



Scheme 3. Synthesis of PH-ddm (a) and oHPMI-ddm (b).

Fig. 2 shows the ^{13}C NMR spectra of benzoxazines, PH-ddm and oHPMI-ddm, in CDCl_3 . The characteristic carbon resonances of the oxazine ring structure for Ar- $\text{CH}_2\text{-N-}$ and $\text{-O-CH}_2\text{-N-}$ in PH-ddm and oHPMI-ddm appear at 50.56 and 79.76 ppm, and 50.97 and 80.16 ppm, respectively. The characteristic carbon resonances of the methylene group in PH-ddm and oHPMI-ddm are observed at 40.27 and 40.30, respectively. In addition, the typical resonance at 134.46 ppm is assigned to the double bond carbon in maleimide functionality in oHPMI-ddm.

The structures of PH-ddm and oHPMI-ddm were also characterized by FT-IR. As shown in Fig. 3, some bands are highlighted, which are used to determine the presence of characteristic groups in PH-ddm and oHPMI-ddm. For instance, the symmetric and antisymmetric stretching modes of carbonyl in maleimide group in oHPMI-ddm are observed at 1709 and 1776 cm^{-1} , respectively [34]. The typical band at 836 cm^{-1} is assigned to the CH wagging of the -CH=CH- in maleimide group, and the band at 692 cm^{-1} is attributed to the $=\text{C-H}$ out-of-plane bending mode for oHPMI-ddm.³⁴ Moreover, the aromatic ether of oxazine ring in both benzoxazines is evidenced by the bands centered at 1226 and 1229 cm^{-1} for PH-ddm and oHPMI-ddm, respectively, which are due to the C-O-C antisymmetric stretching modes [35]. Furthermore, the oxazine ring related modes for PH-ddm and oHPMI-ddm are observed at 946 and 920 cm^{-1} , respectively [36]. Therefore, all the above results from the structural analyses are consistent with the successful synthesis of the anticipated benzoxazine monomers.

3.2. Polymerization and thermal cyclization behaviors of the ortho-maleimide functional bisbenzoxazine

The polymerization profile of oHPMI-ddm was investigated by DSC as shown in Fig. 4. Herein, two counterparts, PH-ddm and DDM-BMI were also investigated by DSC, which are introduced to gain better insights into the polymerization behaviors of oHPMI-ddm. Notably, oHPMI-ddm possesses two polymerizable structure characteristics, including the oxazine ring in PH-ddm and the maleimide functionality in DDM-BMI. Thus, the introduction of both counterparts in this study can give better understanding of the role of oxazine ring and maleimide on the polymerization processes in oHPMI-ddm.

As shown in Fig. 4, among the three monomers studied, oHPMI-ddm shows the lowest melting peak temperature at $105\text{ }^\circ\text{C}$, followed by PH-ddm ($125\text{ }^\circ\text{C}$), and finally DDM-BMI showing the highest endothermic peak temperature at $159\text{ }^\circ\text{C}$. Interestingly, the combination of oxazine

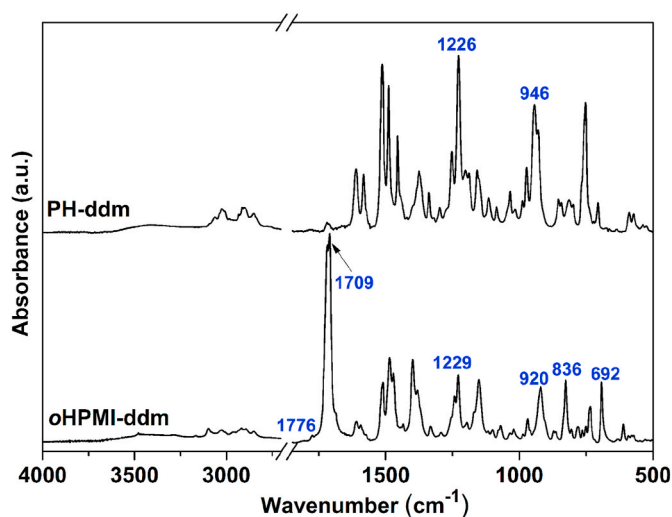


Fig. 3. FT-IR spectra of PH-ddm and oHPMI-ddm.

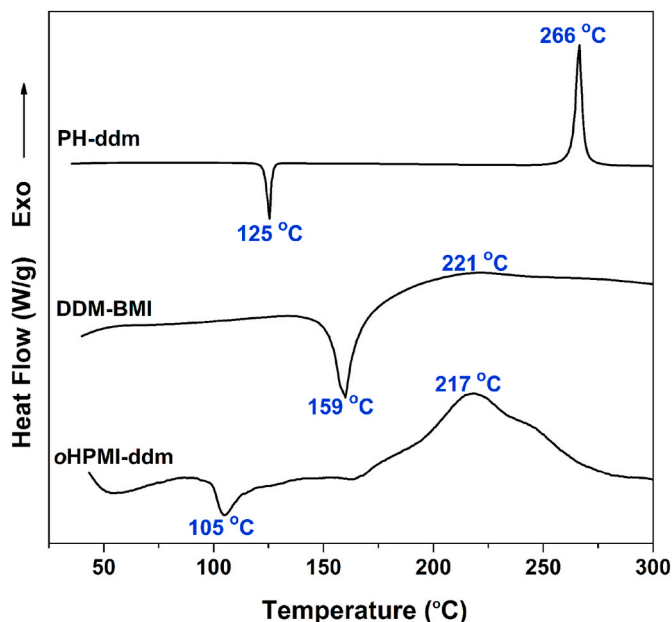


Fig. 4. DSC thermograms of PH-ddm, DDM-BMI and oHPMI-ddm.

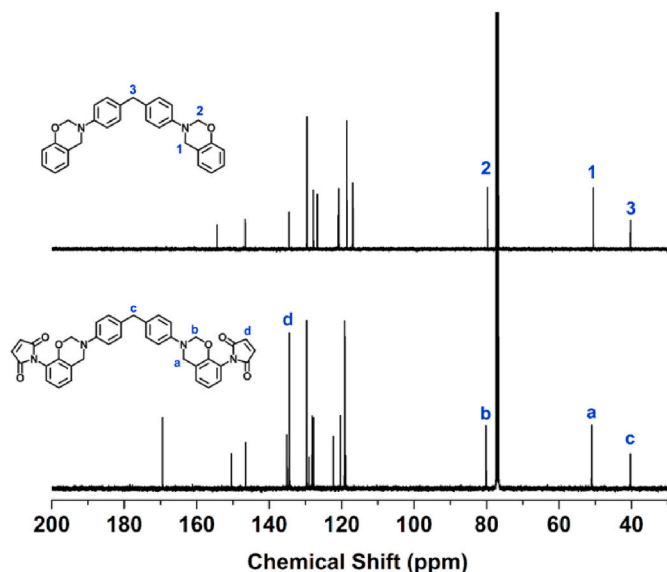


Fig. 2. ^{13}C NMR spectra of PH-ddm and oHPMI-ddm in CDCl_3 .

ring and maleimide group in the same compound significantly decreases the molecular interactions in the thermosetting system. This is of great interest, as oHPMI-ddm exhibits excellent processability potential by taking its low melting temperature and wide processing window ($>110\text{ }^\circ\text{C}$) into consideration. Besides the polymerization behaviors of PH-ddm, DDM-BMI and oHPMI-ddm were also tested by DSC. The exotherm that is attributed to the polymerization of oHPMI-ddm has its maximum located at $217\text{ }^\circ\text{C}$, which is much lower than that of PH-ddm ($266\text{ }^\circ\text{C}$). Particularly, the incorporation of maleimide group in benzoxazine greatly lowers the initial polymerization temperature. In the case of DDM-BMI, a very broad exothermic peak centered at $221\text{ }^\circ\text{C}$ is observed. It should be pointed out that the initial polymerization temperature of maleimide is much lower than oxazine ring as observed from the DSC thermograms of PH-ddm and DDM-BMI. In the oHPMI-ddm thermogram, the very sharp polymerization exotherm observed at $266\text{ }^\circ\text{C}$ in PH-ddm has totally disappeared and seems to have overlapped with the broad exotherm of maleimide. This indicates that the significant reduction of the polymerization temperature for oHPMI-ddm should be attributed to the low starting polymerization temperature of

maleimide functionality. Moreover, oHPMI-ddm shows multiple exotherms rather than a singlet as other reported benzoxazine monomers [14,15]. Quite often, benzoxazines with multiple polymerization mechanisms exhibit a single exothermic peak despite having different polymerization temperatures that correspond to each mechanism. The current system also shows a similar trend of joining two polymerization behaviors into one general polymerization temperature range, possibly due to the acceleration of the benzoxazine polymerization via the exothermic heat generated by the maleimide moieties; however, there are some complications as seen in weak, but multiple peaks heavily overlapped.

DSC measurements at heating rates of 2, 5, 10, 15 and 20 °C/min were also carried out to calculate the activation energy (E_a) of the polymerization reaction of PH-ddm and oHPMI-ddm (Figs. S2 and S3). The activation energy values for both benzoxazines were calculated via the Kissinger and modified Ozawa theories [37,38], using the equations as follows:

$$\text{Kissinger equation: } \ln\left(\frac{\beta}{T_p^2}\right) = \ln\left(\frac{AR}{E_a}\right) - \frac{E_a}{RT_p} \quad (1)$$

$$\text{Modified Ozawa equation: } \ln \beta = -1.052 \frac{E_a}{RT_p} + C \quad (2)$$

Where β is the heating rate, T_p is the maximum of the exotherm, A represents the frequency factor, R is the gas constant, and C is a constant. As shown in Fig. 5, the plots exhibit straight lines based on the two theories for both benzoxazines. The E_a values calculated from the slope of Kissinger and Ozawa's plots for PH-ddm are 125.1 and 127.6 kJ/mol, respectively. In comparison, the E_a values of oHPMI-ddm are obtained to be 103.3 and 105.7 kJ/mol, respectively, as summarized in Table 1.

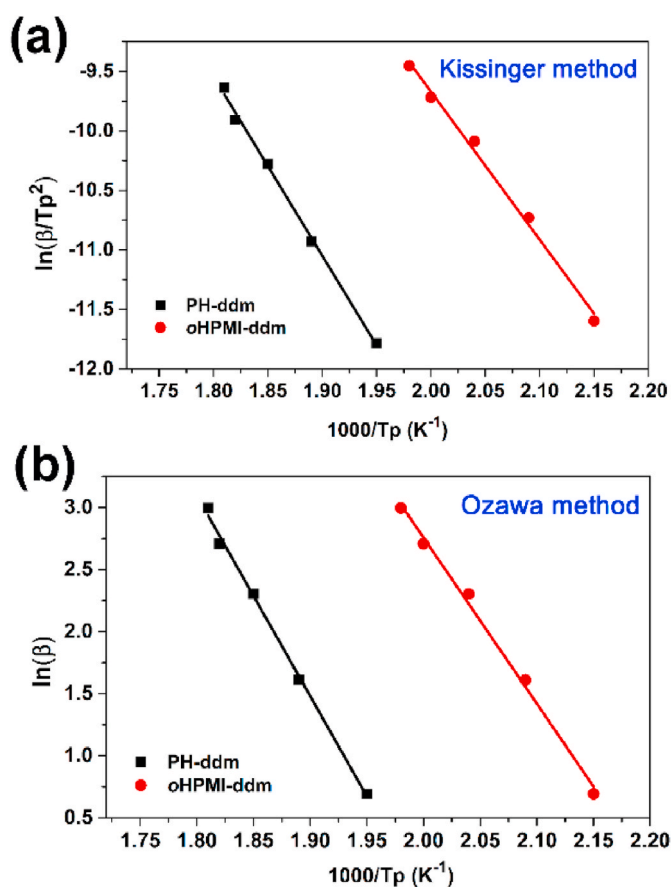


Fig. 5. Representations of the Kissinger (a) and Ozawa (b) theories for the calculation of E_a values for PH-ddm and oHPMI-ddm.

Table 1

E_a values of PH-ddm and oHPMI-ddm calculated by the Kissinger and Ozawa Theories.

Sample	Kissinger	Ozawa
	E_a (kJ/mol)	E_a (kJ/mol)
PH-ddm	125.1	127.6
oHPMI-ddm	103.3	105.7

The E_a values calculated for oHPMI-ddm are much lower than those of PH-ddm. In other words, oHPMI-ddm is comparatively easy to activate towards its polymerization. The only structural difference between PH-ddm and oHPMI-ddm is the existence of maleimide group at the *ortho* position with respect to the oxygen in oxazine ring in oHPMI-ddm. This is quite unexpected since the carbonyl group of the maleimide moiety does not possess an obvious labile proton that can hydrogen bond to the oxazine ring. Previously, all the smart *ortho*-functional benzoxazine monomers that showed low polymerization temperatures were structured with the functional groups that were capable of hydrogen bond formation with the oxazine ring either as the 5-membered or 6-membered intramolecular hydrogen bonds [39,40]. However, it is well-known that maleimide group can form a keto-enol tautomer with the hydrogen atom migration [41,42]. The enol form of the tautomer can potentially form a weak hydrogen bond as it can have an intramolecular 7-membered ring configuration. Admittedly, the 7-membered ring is not as stable as the 6-membered ring. Yet, an intramolecular 5-membered ring, which is smaller than the stable 6-membered ring, has been shown to form a hydrogen bond and cause lowering of the oxazine ring polymerization temperature. Furthermore, the 7-membered ring has been shown to form a hydrogen bond as well [43,44]. Fig. S4 shows the FT-IR spectra of bismaleimide without oxazine ring, DDM-BMI, and its benzoxazine counterpart, oHPMI-ddm in the expanded region of 1800–1000 cm⁻¹. Due to the symmetric configuration of the benzene ring to which the maleimide is attached, the band contour of the imide group is relatively symmetric. However, when the oxazine ring is attached, due to the possible 7-membered intramolecular interaction, one carbonyl is less conjugated and another is more double bond nature, resulting in widening of carbonyl frequencies. As a result, the carbonyl band is clearly separated into two peaks. This observation is consistent with the hypothesized intramolecular interaction of oHPMI-ddm. All these advantages observed in polymerization behaviors are largely due to the combination of oxazine ring and maleimide in the same benzoxazine compound and the weak interactions between these moieties via a 7-membered intramolecular hydrogen bond.

In order to qualitatively investigate the structural transformation during the polymerization of oHPMI-ddm, *in situ* FT-IR analyses were then performed. Ordinarily, the bands corresponding to the C–O–C antisymmetric stretching (~1230 cm⁻¹) and benzoxazine (~940 cm⁻¹) are used to monitor the ring-opening polymerization of benzoxazine rings [35,36]. As can be seen in Figs. S5 and 6, both characteristic bands decrease as the heating temperature increase, and fully disappear at 220 °C for PH-ddm and 240 °C for oHPMI-ddm, respectively. The bands due to the CH wagging of the vinylene group from maleimide in oHPMI-ddm undergo substantial decrease at higher temperature, suggesting the polymerization of maleimide group. These results therefore confirm that the polymerization of oHPMI-ddm has two parallel processes, the polymerization of maleimide and ring-opening polymerization of oxazine ring.

Previous studies reported that *ortho*-imide polybenzoxazines can form a benzoxazole by further thermal treatment, leading to another class of thermosets, specifically, cpBOs.²⁹ Taking advantage of the remarkable molecular design flexibility of *ortho*-imide benzoxazine resins, various *ortho*-imide functional benzoxazines have been synthesized for preparing polybenzoxazoles via an intramolecular cyclization between neighboring hydroxyl and phthalimide [45,46]. However, the

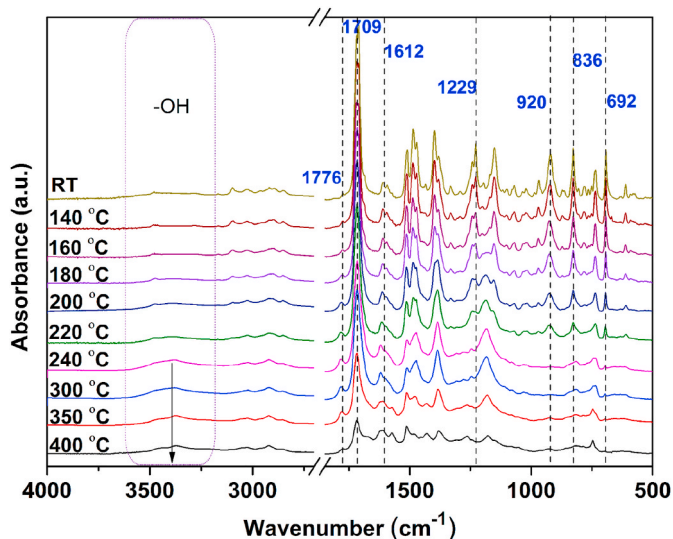


Fig. 6. FT-IR spectra of oHPMI-ddm after various thermal treatments at the designated temperature for 1 h.

thermal cyclization between neighboring maleimide and hydroxyl has never been investigated. Since maleimide belongs to the imide family, we reasonably predict that oHPMI-ddm could undergo a unique structural transformation at elevated temperatures. Thus, *in situ* FT-IR analyses at higher temperatures were further conducted for oHPMI-ddm. As seen from Fig. 6, the typical carbonyl bands in maleimide occur at 1776 and 1709 cm^{-1} , and the -OH band around 3400 cm^{-1} gradually decrease when heated from 240 to 400 °C. Meanwhile, the typical band at 1618 cm^{-1} (C=N stretching) for benzoxazole gradually increases [31, 32]. The *in situ* FT-IR spectra of this newly obtained *ortho*-maleimide-functional bisbenzoxazine is practically identical to those reported for cPBOs achieved via the cyclization of phthalimide hydroxyl and from *ortho*-imide benzoxazines, indicating the possibility to prepare high performance cPBOs based on *ortho*-maleimide benzoxazine resins.

The structural transformation from benzoxazine, oHPMI-ddm, to cross-linked polybenzoxazole was further supported by solid-state ^{13}C NMR as shown in Fig. 7. In accordance with the ^{13}C NMR result of oHPMI-ddm in solution, the typical solid ^{13}C resonances of the oxazine ring can be assigned to resonances around 50 and 80 ppm for Ar-CH₂-N-

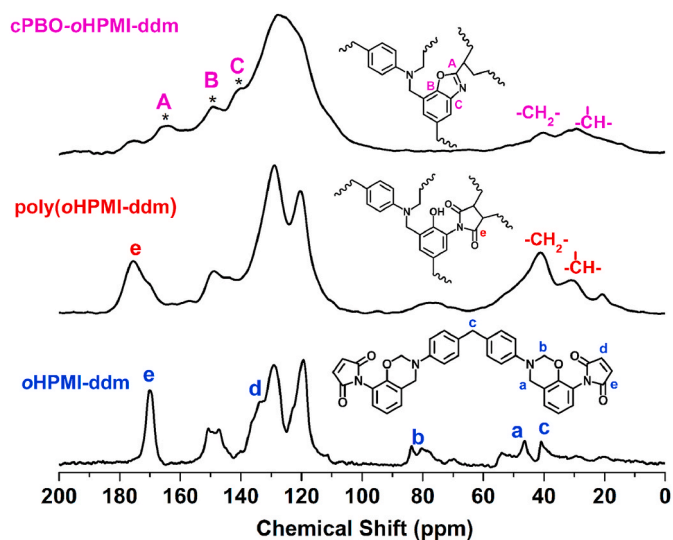
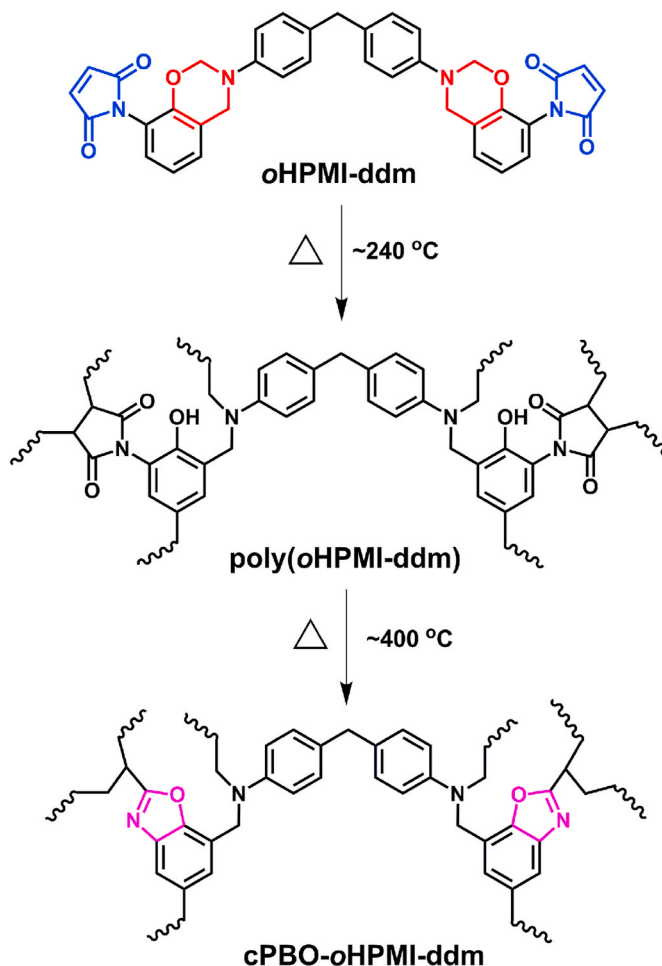


Fig. 7. Solid-state ^{13}C NMR spectra of oHPMI-ddm, poly(oHPMI-ddm) and cPBO-oHPMI-ddm.

and -O-CH₂-N-, respectively. In addition, the signal of the maleimide carbon of -CH=CH- is located around 134 ppm. The spectra for poly(oHPMI-ddm) and cPBO-oHPMI-ddm exhibited obvious differences compared with that of oHPMI-ddm. The carbon resonances of oxazine ring and maleimide in oHPMI-ddm have fully disappeared in the spectra of poly(oHPMI-ddm) and cPBO-oHPMI-ddm, multiple broad resonances, which can be assigned to the carbons in methylene and methylidene of poly(oHPMI-ddm), appeared in the range from 20 to 60 ppm. These variations indicate the completion of ring-opening polymerization of oxazine ring and cross-linking of maleimide in poly(oHPMI-ddm). Moreover, the new carbon resonances at 163, 149 and 141 ppm in the spectrum of cPBO-oHPMI-ddm, which are assigned to the carbon resonances in benzoxazole moiety, are well resolved [27,47,48]. The assignment for benzoxazole group can be further supported since no benzoxazole carbons can be observed for the samples of PH-ddm and DDM-BMI after thermal treatment at 400 °C as shown in Figs. S6 and S7. Meanwhile, the characteristic carbon resonance from carbonyl in poly(oHPMI-ddm) decreases after the further treatment for obtaining cPBO-oHPMI-ddm. As a result, the conversion from polybenzoxazine to polybenzoxazole is around 75% by integrating peaks A and e in the spectrum of cPBO-oHPMI-ddm. These NMR spectral differences among the benzoxazine monomer, polybenzoxazine and finally obtained thermoset are a strong evidence of the proposed benzoxazole formation from *ortho*-maleimide-functional benzoxazine and in accordance with the conclusion obtained from the FT-IR analyses. Therefore, we propose a structural transformation behavior for oHPMI-ddm as shown in Scheme 4.



Scheme 4. Polymerization of oHPMI-ddm Forming Polybenzoxazine and Subsequent Structural Transformation into cPBO.

3.3. Thermal properties of thermosets

DMA measurements were carried out for poly(PH-ddm), poly(oHPMI-ddm) and cPBO-oHPMI-ddm as shown in Fig. 8. Herein, good DMA samples of poly(DDM-BMI) were difficult to prepare due to the brittleness of the thermosets based on pure DDM-BMI. It is not unexpected as many previous literatures have pointed out this shortcoming of pure bismaleimide resin, and thereby bismaleimide thermosetting resins are always processed by adding other additives [7–13]. Nevertheless, we found a reported T_g value (222 °C) of poly(DDM-BMI) obtained by an unknown method, which could be used as a guideline for researchers [13]. As shown in the figure, poly(PH-ddm) and poly(oHPMI-ddm) show T_g temperatures at 214 and 306 °C, respectively. Obviously, the T_g value of poly(oHPMI-ddm) is much higher than poly(PH-ddm), poly(DDM-BMI) as well as the polymerization temperature of itself. The additional cross-linking reaction based on the C=C group in maleimide group in oHPMI-ddm increases the overall cross-link density of the networks, thereby greatly increasing the T_g temperature of poly(oHPMI-ddm). In addition, cPBO-oHPMI-ddm exhibits no T_g below 400 °C as also shown in Fig. 8, indicating its potential application in a very high temperature environment. Specifically, cPBO-oHPMI-ddm shows a stable, constant storage modulus up to 300 °C due to the presence of rigid benzoxazole moiety, which is a stiffer structure than that of poly(oHPMI-ddm). Of particular interest is the readily processable precursor benzoxazine resin, having the melting endotherm at 105 °C. It is important to point out that this low melting temperature was observed despite having the high monomer purity as shown in ^1H NMR spectrum in Fig. 1 and elemental analysis result without the presence of hydroxyl impurities which in an impure sample act as effective initiators. Such characteristics are very different from other reported cPBO precursors of *ortho*-imide functional benzoxazine monomers, which all showed high melting peak temperatures greater than 200 °C [29,46].

The thermal stability of poly(PH-ddm), poly(DDM-BMI), poly(oHPMI-ddm) and cPBO-oHPMI-ddm were studied by TGA under a N_2 atmosphere. The weight loss and derivative weight loss curves are depicted in Fig. 9. Notably, poly(DDM-BMI) shows very high thermal stability during the thermal treatment below 450 °C, while both polybenzoxazines, poly(PH-ddm) and poly(oHPMI-ddm), exhibit weight-loss from 300 to 450 °C. The initial weight loss at this stage for polybenzoxazines is mainly due to the initial decomposition of defect groups [49]. Hence, the thermal properties, in terms of T_{d5} (5% weight loss temperature) and T_{d10} (10% weight loss temperature) for poly(oHPMI-ddm) manifest a trade-off between poly(PH-ddm), poly(DDM-BMI). On the other hand, both polybenzoxazines show broad derivative peaks as shown in Fig. 9b, while poly(DDM-BMI) exhibits a much higher

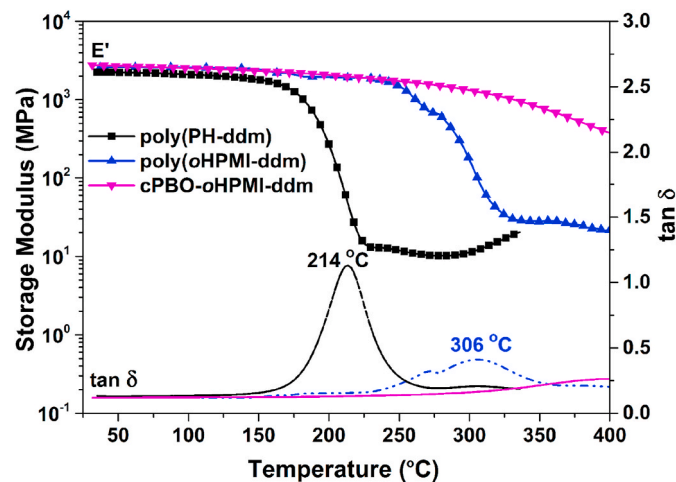


Fig. 8. Dynamic mechanical spectra of poly(PH-ddm), poly(oHPMI-ddm) and cPBO-oHPMI-ddm.

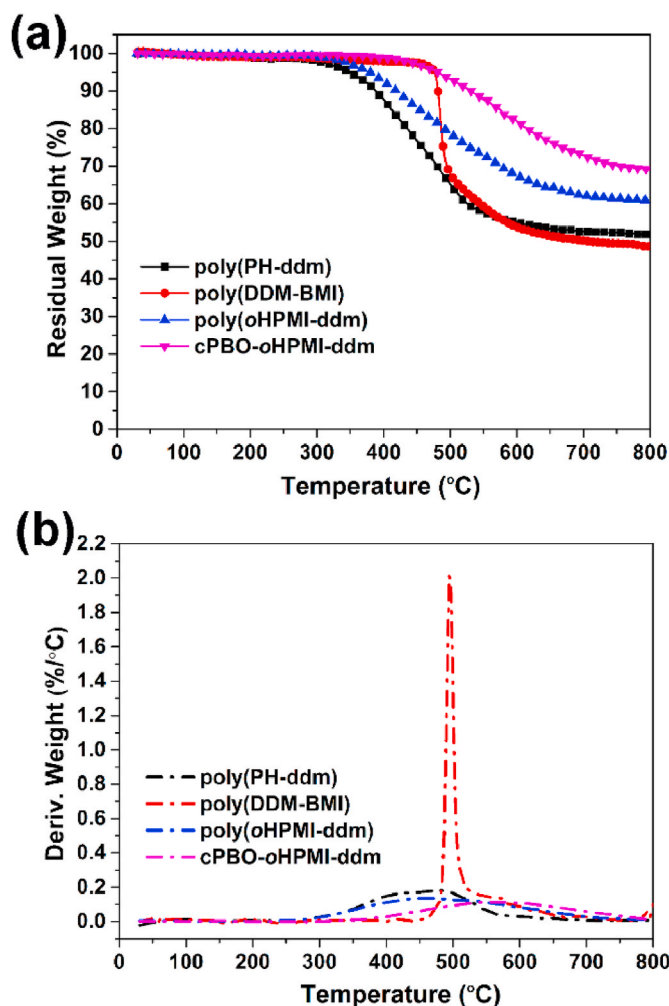


Fig. 9. TGA thermograms (a) and derivative weight loss curves (b) of poly(PH-ddm), poly(DDM-BMI), poly(oHPMI-ddm) and cPBO-oHPMI-ddm.

weight-loss rate around 500 °C. The effect of this sharp decomposition behavior will be discussed in the next section.

cPBO-oHPMI-ddm possesses outstanding thermal stability with very high T_{d5} value of 482 °C and T_{d10} of 533 °C, respectively, as a consequence of the benzoxazole formation. In addition, cPBO-oHPMI-ddm shows very high Y_c value of 69%. The thermal property data of all the thermosets obtained in this study are summarized in Table 2. The data indicates the very high thermal stability of the freshly obtained *ortho*-maleimide functional bisbenzoxazine based thermosets.

3.4. Flammability of thermosets

The heat release capacity (HRC) and total heat release (THR) values are used to evaluate the flammability of thermosets [50,51], which are obtained from MCC in the current study. Milligram size samples of poly(PH-ddm), poly(DDM-BMI), poly(oHPMI-ddm) and cPBO-oHPMI-ddm were measured at 1 K/s over the temperature range of 100–750 °C. As shown in Fig. 10, MCC spectra of poly(DDM-BMI), poly(PH-ddm), poly(oHPMI-ddm) and cPBO-oHPMI-ddm reveal HRC values of 169.7, 66.6, 22.7 and 7.3 $\text{Jg}^{-1}\text{K}^{-1}$, respectively. The highest HRC value of bismaleimide based thermoset is due to the highest decomposition rate around 500 °C. Besides, poly(PH-ddm), poly(DDM-BMI), and poly(oHPMI-ddm) exhibit THR values of 9.4, 8.4 and 5.3 KJg^{-1} , while cPBO-oHPMI-ddm shows a much lower THR value of 2.3 KJg^{-1} . In general, lower the values of HRC and THR suggest higher flame resistance. The HRC values of bisbenzoxazine derived thermosets are much lower than the other 86

Table 2
Thermal, Fire and Dielectric-Related Properties of poly(PH-ddm), poly(DDM-BMI), poly(oHPMI-ddm) and cPBO-oHPMI-ddm.

Sample	T_g (°C)	T_{d5} (°C)	T_{d10} (°C)	Y_c (wt.%)	HRC ($Jg^{-1}K^{-1}$)	THR (KJg^{-1})	k (at 1 MHz)
poly(PH-ddm)	214	351	387	52	66.6	9.4	3.30
poly(DDM-BMI)	222 ^a	475	480	49	169.7	8.4	3.15
poly(oHPMI-ddm)	306	380	418	61	22.7	5.3	2.85
cPBO-oHPMI-ddm	–	482	533	69	7.3	2.3	2.49

^a Data was obtained from Ref. [13].

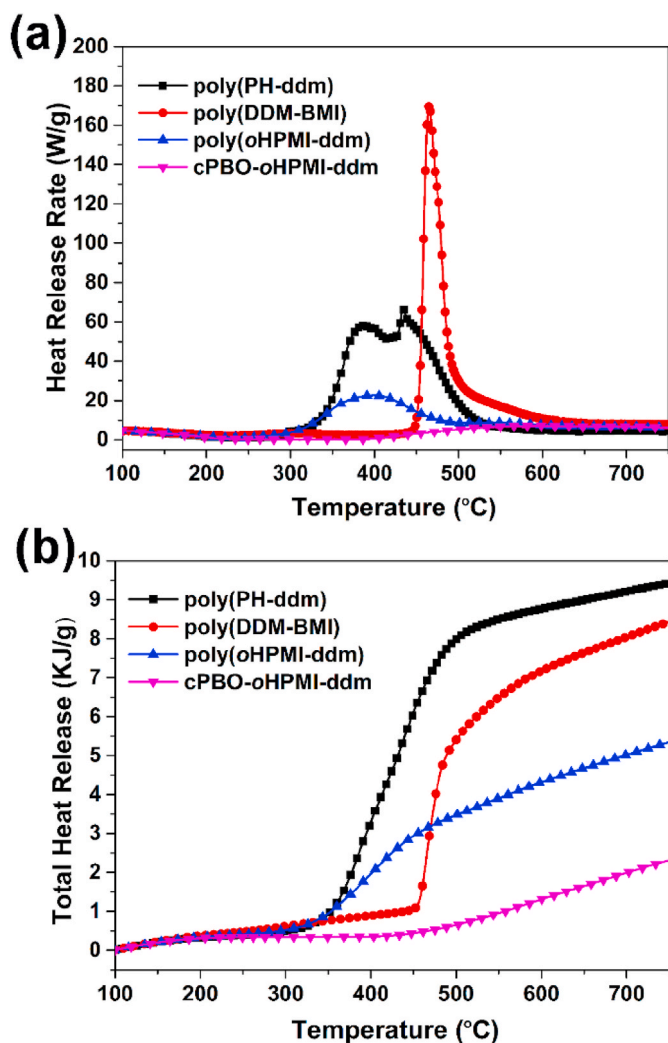


Fig. 10. Heat release rate (HRR) (a) and total heat release (THR) (b) versus temperature for poly(PH-ddm), poly(DDM-BMI), poly(oHPMI-ddm) and cPBO-oHPMI-ddm.

polymers reported by Walters and Lyon [52]. Particularly, the combination of oxazine ring and maleimide in the same molecular structure leads to a substantial HRC reduction. Hence, *ortho*-maleimide functional bisbenzoxazine based thermosets also extend opportunities for applications that benefit from low flammability. The extremely low HRC of cPBO-oHPMI-ddm at 5.3 KJg^{-1} is particularly noteworthy. Considering all the polymers reported by Lyon and others [53–56], this polymer showed the lowest HRC, clearly demonstrating an extremely non-combustible nature. Polymers exhibiting a HRC less than 100 are considered non-ignitable and will pass strict Federal Aviation Administration requirements for the heat release rate of materials used for commercial aircraft cabins [56].

Despite having good thermal stability below the decomposition temperature, the sharp decomposition and heat release behavior of poly

(DDM-BMI) are significant disadvantages when considering flammability. Having a very narrow temperature range of the heat release curve contributes to the sudden and significant increase in the flaming temperature. On the other hand, the broadening of the derivative peaks for polybenzoxazines indicates a slow decomposition rate over a wide temperature range, which, in general, is beneficial for reduced flammability [57,58]. Therefore, the advantages of combining benzoxazine and maleimide moieties in the same benzoxazine monomer is at least two-folds: firstly, enhancing the thermal stability of the initial weight-loss stage though the cross-linked network formed by maleimide group; secondly, improving the fire retardancy via the cross-linked network contributed from oxazine ring.

3.5. Dielectric properties of thermosets

The dielectric constants of thermoset films were calculated by the capacitance method applying the following equation:

$$k = \frac{Cl}{Ak_0} \quad (3)$$

Herein, C is the capacitance of each thermoset, A is the surface area of the silver coated samples, l is the thickness of the thermoset film samples, and k_0 is the vacuum dielectric constant ($8.854 \times 10^{-12} \text{ F m}^{-1}$).

As shown in Fig. 11a, the k values at 1 MHz of the thermosets, poly(PH-ddm), poly(DDM-BMI), poly(oHPMI-ddm) and cPBO-oHPMI-ddm, are 3.30, 3.15, 2.85 and 2.49 respectively. The k values of poly(oHPMI-ddm) is much lower than poly(PH-ddm), poly(DDM-BMI). The introduction of maleimide group into benzoxazine thermosetting system can significantly reduce the dielectric constants of the corresponding thermoset. The additional crosslinking network may lower the dielectric constant by increasing the free volume in thermoset structures. Additionally, the benzoxazole formation between the maleimide and hydroxyl group converts the polarizable phenolic hydroxyl into less polarizable benzoxazole functionality, resulting in a lower dielectric constant of cPBO-oHPMI-ddm. Particularly, the low dielectric constant of *ortho*-maleimide based thermosets is comparable to the values of other commercially available low- k polymeric materials, such as cyanate esters and polyimides [59,60].

Fig. 11b shows the dielectric loss ($\tan\delta$) of poly(PH-ddm), poly(DDM-BMI), poly(oHPMI-ddm) and cPBO-oHPMI-ddm as a function of the frequency within the range of 100 Hz to 1 MHz. The dielectric loss was found to vary from 0.0060 to 0.0063 for cPBO-oHPMI-ddm. In general a relatively low value of dielectric loss is always required for the application as interlayer dielectric materials [61]. In a modern electronic communication, the communication frequency continues to increase due to the need of conveying a large amount of messages. Therefore, the results from dielectric measurements show that the newly developed *ortho*-maleimide bisbenzoxazine is suitable for various applications, such as in the advanced electronics, automotive and aerospace fields.

4. Conclusion

In summary, we have successfully synthesized an *ortho*-maleimide functional bisbenzoxazine resin, which features advantages originating from both benzoxazine and maleimide moieties, and further synergistic effect of having both moieties in the same molecule at the *ortho*-position.

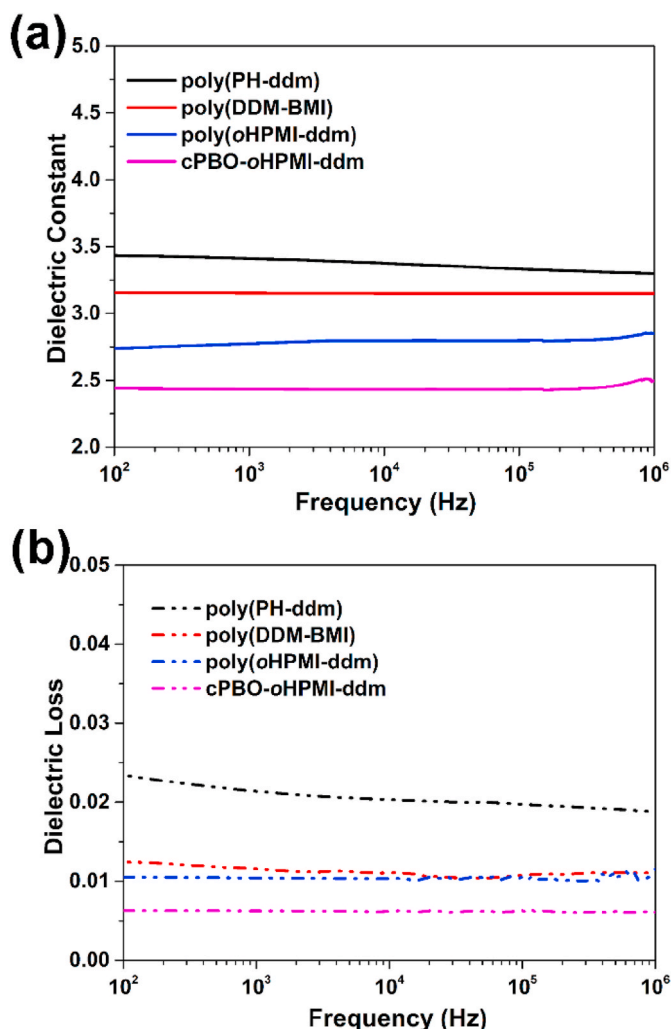


Fig. 11. Dielectric constant (a) and dielectric loss (b) versus frequency of poly (PH-ddm), poly(DDM-BMI), poly(oHPMI-ddm) and cPBO-oHPMI-ddm at room temperature.

The cross-linked polybenzoxazine based on this newly obtained benzoxazine was firstly found to form a more thermally stable cross-linked polybenzoxazole through the cyclization between neighboring hydroxyl and maleimide. In addition, the corresponding thermosets exhibits a tremendously unusual set of combined beneficial properties fully desirable in all thermosetting resins, including high thermal stability, excellent flame resistance and low dielectric constant. Notably, the cPBO derived from the *ortho*-maleimide functional bisbenzoxazine monomer showed low dielectric constants, less than 2.52, within the frequency range of 100 Hz to 1 MHz, and extremely high thermal stability with a glass transition temperature over 400 °C and a T_{d5} of 482 °C. Therefore, this work paves a smart approach for the development of very high-performance thermosets based on combining different moieties in the same benzoxazine monomer.

Declaration of competing interest

The authors declare that they have no known competing financial interests or personal relationships that could have appeared to influence the work reported in this paper.

Acknowledgements

The authors thank the National Natural Science Foundation of China

(52073125 and 51603093) for financial support.

Appendix A. Supplementary data

Supplementary data to this article can be found online at <https://doi.org/10.1016/j.polymer.2021.123703>.

References

- [1] R.J. Iredale, C. Ward, I. Hamerton, Modern advanced in bismaleimide resin technology: a 21st century perspective on the chemistry of addition polyimides, *Prog. Polym. Sci.* 69 (2017) 1–21.
- [2] H.D. Stenzenberger, Addition polyimides, *Adv. Polym. Sci.* 117 (1994) 165–220.
- [3] Y.L. Liu, J.M. Yu, C.I. Chou, Preparation and properties of novel benzoxazine and polybenzoxazine with maleimide groups, *J. Polym. Sci. Pol. Chem.* 42 (2004) 5954–5963.
- [4] H. Ishida, S. Ohba, Synthesis and characterization of maleimide and norbornene functionalized benzoxazines, *Polymer* 46 (2005) 5588–5595.
- [5] X. Wang, D.Y. Chen, W.H. Ma, X.J. Yang, L.D. Lu, Polymerization of bismaleimide and maleimide catalyzed by nanocrystalline titania, *J. Appl. Polym. Sci.* 71 (1999) 665–669.
- [6] B.A. Rozenberg, E.A. Dzhavadyan, R. Morgan, E. Shin, High-performance bismaleimide materials: cure kinetics and mechanism, *Polym. Adv. Technol.* 13 (2002) 837–844.
- [7] S. Takeda, H. Kakiuchi, Toughening bismaleimide resins by reactive liquid rubbers, *J. Appl. Polym. Sci.* 35 (1988) 1351–1366.
- [8] T. Iijima, N. Hayashi, T. Oyama, M. Tomoi, Modification of bismaleimide resin by soluble poly(ester imide) containing trimellitimidate moieties, *Polym. Int.* 53 (2004) 1417–1425.
- [9] H. Qin, P.T. Mather, J.B. Baek, L.S. Tan, Modification of bisphenol-A based bismaleimide resin (BPA-BMI) with an allyl-terminated hyperbranched polyimide (AT-PAEKI), *Polymer* 47 (2006) 2813–2821.
- [10] X.Y. Liu, Y.F. Yu, S.J. Li, Study on cure reaction of the blends of bismaleimide and dicyanate ester, *Polymer* 47 (2006) 3767–3773.
- [11] F. Liu, Z. Wang, C.L. Lü, L.X. Gao, M.X. Ding, Gamma ray irradiation-initiated copolymerization of a binary casting system involving DPBMIn and vinylpyrrolidone, *Macromol. Mater. Eng.* 290 (2010) 726–732.
- [12] Y.Q. Wang, K.C. Kou, L.H. Zhuo, H. Chen, Y. Zhang, G.L. Wu, Thermal, mechanical and dielectric properties of BMI modified by the bis allyl benzoxazine, *J. Polym. Res.* 22 (2015) 51.
- [13] T. Takeichi, Y. Saito, T. Agag, H. Muto, T. Kawauchi, High-performance polymer alloys of polybenzoxazine and bismaleimide, *Polymer* 49 (2008) 1173–1179.
- [14] H. Ishida, T. Agag, *Handbook of Benzoxazine Resins*, Elsevier, Amsterdam, 2011.
- [15] H. Ishida, P. Froimowicz, *Advanced and Emerging Polybenzoxazine Science and Technology*, Elsevier, Amsterdam, 2017.
- [16] X. Ning, H. Ishida, Phenolic materials via ring-opening polymerization: synthesis and characterization of bisphenol-A based benzoxazines and their polymers, *J. Polym. Sci., Part A: Polym. Chem.* 32 (1994) 1121–1129.
- [17] N.N. Ghosh, B. Kiskan, Y. Yagci, Polybenzoxazines-new high performance thermosetting resins: synthesis and properties, *Prog. Polym. Sci.* 32 (2007) 1344–1391.
- [18] B. Kiskan, Adapting benzoxazine chemistry for unconventional applications, *React. Funct. Polym.* 129 (2018) 76–88.
- [19] H. Ishida, D.J. Allen, Physical and mechanical characterization of near-zero shrinkage polybenzoxazines, *J. Polym. Sci., Part B: Polym. Phys.* 34 (1996) 1019–1030.
- [20] K. Zhang, Y. Liu, H. Ishida, Polymerization of an AB-type benzoxazine monomer toward different polybenzoxazine networks: when diels-alder reaction meets benzoxazine chemistry in a single-component resin, *Macromolecules* 52 (2019) 7386–7395.
- [21] K. Zhang, X. Yu, S.W. Kuo, Outstanding dielectric and thermal properties of main chain-type poly(benzoxazine-co-imide-co-siloxane)-based cross-linked networks, *Polym. Chem.* 10 (2019) 2387–2396.
- [22] S.N. Kolanadiyil, M. Minami, T. Endo, Implementation of meta-positioning in tetrafunctional benzoxazines: synthesis, properties, and differences in the polymerized structure, *Macromolecules* 53 (2020) 6866–6886.
- [23] M. Goto, T. Yajima, M. Minami, H. Sogawa, F. Sando, Synthesis and cross-linking of a benzoxazine-containing anthracene moiety: thermally stable photoluminescent benzoxazine resin, *Macromolecules* 53 (2020) 6640–6648.
- [24] C.F. Wang, Y.C. Su, S.W. Kuo, C.F. Huang, Y.C. Sheen, F.C. Chang, Low-surface-free-energy materials based on polybenzoxazines, *Angew. Chem. Int. Ed.* 45 (2006) 2248–2251.
- [25] S.W. Kuo, Y.C. Wu, C.F. Wang, K.U. Jeong, Preparing low-surface-energy polymer materials by minimizing intermolecular hydrogen-bonding interactions, *J. Phys. Chem. C* 113 (2009) 20666–20673.
- [26] J. Wu, Y. Xi, G.T. Mccandless, Y. Xie, R. Menon, Y. Patel, R. Menon, Y. Patel, D. J. Yang, S.T. Iacono, B.M. Novak, Synthesis and characterization of partially fluorinated polybenzoxazine resins utilizing octafluorocyclopentene as a versatile building block, *Macromolecules* 48 (2015) 6087–6095.
- [27] T. Agag, J. Liu, R. Graf, H.W. Spiess, H. Ishida, Benzoxazole resin: a novel class of thermoset polymer via smart benzoxazine resin, *Macromolecules* 45 (2012) 8991–8997.

- [28] K. Zhang, J. Liu, H. Ishida, An ultrahigh performance cross-linked polybenzoxazole via thermal conversion from poly(benzoxazine amic acid) based on smart o-benzoxazine chemistry, *Macromolecules* 47 (2014) 8674–8681.
- [29] K. Zhang, J. Liu, S. Ohashi, X. Liu, Z. Han, H. Ishida, Synthesis of high thermal stability polybenzoxazoles via *ortho*-imide-functional benzoxazine monomers, *J. Polym. Sci., Part A: Polym. Chem.* 53 (2015) 1330–1338.
- [30] Z. Deliballi, B. Kiskan, Y. Yagci, Advanced polymers from simple benzoxazines and phenols by ring-opening addition reactions, *Macromolecules* 53 (2020) 2354–2361.
- [31] T. Fukumaru, T. Fujigaya, N. Nakashima, Extremely high thermal resistive poly(p-phenylene benzobisoxazole) with desired shape and from a newly synthesized soluble precursor, *Macromolecules* 45 (2012) 4247–4253.
- [32] T. Fukumaru, Y. Saegusa, F. Fujigaya, N. Nakashima, Fabrication of poly(p-phenylenebenzobisoxazole) film using a soluble poly(o-alkoxyphenylamide) as the precursor, *Macromolecules* 47 (2014) 2088–2095.
- [33] K. Zhang, Y.Q. Liu, C.J. Evans, S.F. Yang, Easily processable thermosets with outstanding performance via smart twisted small-molecule benzoxazines, *Macromol. Rapid Commun.* 41 (2020) 1900625.
- [34] L. Jin, T. Agag, H. Ishida, Bis(benzoxazine-maleimide)s as a novel class of high performance resin: synthesis and properties, *Eur. Polym. J.* 46 (2010) 354–363.
- [35] J. Dunkers, H. Ishida, Vibrational assignments of 3-Alkyl-3, 4-Dihydro-6-Methyl-2H-1,3-benzoxazines in the fingerprint region, *Spectrochim. Acta* 51A (1995) 1061–1074.
- [36] L. Han, D. Iguchi, P. Gil, T.R. Heyl, V.M. Sedwick, C.R. Arza, S. Ohashi, D.J. Lacks, H. Ishida, Oxazine ring-related vibrational modes of benzoxazine monomers using fully aromatically substituted, Deuterated, ¹⁵N isotope exchanged, and oxazine-ring-substituted compounds and theoretical calculations, *J. Phys. Chem. A* 121 (2017) 6269–6282.
- [37] H.E. Kissinger, Reaction kinetics in differential thermal analysis, *Anal. Chem.* 29 (1957) 1702–1706.
- [38] T. Ozawa, Kinetics of non-isothermal crystallization, *Polymer* 12 (1971) 12150–12158.
- [39] P. Froimowicz, K. Zhang, H. Ishida, Intramolecular hydrogen bonding in benzoxazines: when structural design becomes functional, *Chem. Eur. J.* 22 (2016) 2691–2707.
- [40] K. Zhang, Y. Liu, M. Han, P. Froimowicz, Smart and sustainable design of latent catalyst-containing benzoxazine-bio-resins and application studies, *Green Chem.* 22 (2020) 1209–1219.
- [41] A. Ackera, H.J. Hofmann, R. Cimiriaglia, On the tautomerism of maleimide and phthalimide derivatives, *J. Mol. Struct.: Theochem.* 315 (1994) 43–51.
- [42] S. Sarker, T. Ash, T. Debnath, A.K. Das, Exploration of tautomerizations of succinimide and maleimide assisted by ammonia and methanol: a theoretical perspective, *Theoret. Chem. Acc.* 138 (2019) 55.
- [43] M. Tamres, S. Searles Jr., Hydrogen bonding abilities of cyclic sulfoxides and cyclic ketones, *J. Am. Chem. Soc.* 81 (1959) 2100–2104.
- [44] Y. Jin, K. Tonan, S. Ikawa, Competitive formation of 10- and 7-membered hydrogen-bonded rings of proline-containing model peptides, *Spectrochim. Acta A Mol. Biomol. Spectrosc.* 58 (2002) 2795–2802.
- [45] A.F.M. El-Mahdy, S.W. Kuo, Direct synthesis of poly(benzoxazine imide) from an *ortho*-benzoxazine: its thermal conversion to highly cross-linked polybenzoxazole and blending with poly(4-vinylphenol), *Polym. Chem.* 9 (2018) 1815–1826.
- [46] K. Zhang, Y.Q. Liu, L. Han, J.Y. Wang, H. Ishida, Synthesis and thermally induced structural transformation of phthalimide and nitrile-functional benzoxazine: toward smart *ortho*-benzoxazine chemistry for low flammability thermosets, *RSC Adv.* 9 (2019) 1526–1535.
- [47] H. Shamsipur, B.A. Dawood, P.M. Budd, P. Bernardo, G. Clarizia, J.C. Jansen, Thermally rearrangeable PIM-polyimides for gas separation membranes, *Macromolecules* 47 (2014) 5595–5606.
- [48] D.F. Sanders, R.L. Guo, Z.P. Smith, Q. Liu, K.A. Stevens, J.E. McGrath, D.R. Paul, B. D. Freeman, Influence of polyimide precursor synthesis route and *ortho*-position functional group on thermally rearranged (TR) polymer properties: conversion and free Volume, *Polymer* 55 (2014) 1636–1647.
- [49] N.K. Sini, T. Endo, Toward elucidating the role of number of oxazine rings and intermediates in the benzoxazine backbone on their thermal characteristics, *Macromolecules* 49 (2016) 8466–8478.
- [50] D.W. Van Krevelen, Some basic aspects of flame resistance of polymeric materials, *Polymer* 16 (1975) 615–620.
- [51] R.N. Walters, R.E. Lyon, Molar group contributions to polymer flammability, *J. Appl. Polym. Sci.* 87 (2003) 548–563.
- [52] R.E. Lyon, R.N. Walters, Pyrolysis combustion flow calorimetry, *J. Anal. Appl. Pyrol.* 71 (2004) 27–46.
- [53] H. Zhang, Fire-safe polymers and polymer composites, in: Technical Report of Federal Aviation Administration, US Department of Transportation, 2004. DOT/FAA/AR-04/11.
- [54] R.E. Lyon, M.L. Janssens, Polymer Flammability, Technical Report of Federal Aviation Administration, US Department of Transportation, 2005. DOT/FAA/AR-05/14.
- [55] R.E. Lyon, L. Speitel, R. Filipczak, R.N. Walters, S. Crowley, S. Stolarov, L. Castelli, M. Ramirez, Fire-smart DDE polymers, in: Technical Report of Federal Aviation Administration, US Department of Transportation, 2006. DOT/FAA/AR-06/12.
- [56] R.E. Lyon, R.N. Walters, S.I. Stolarov, Thermal analysis of flammability, *J. Therm. Anal. Calorim.* 89 (2007) 441–448.
- [57] F. Shan, S. Ohashi, A. Erlichman, H. Ishida, Non-flammable thiazole-functional monobenzoxazines: synthesis, polymerization, thermal and thermomechanical properties, and flammability studies, *Polymer* 157 (2018) 38–49.
- [58] J. Wang, M. Wu, W. Liu, S. Yang, S. Bai, Q. Ding, Y. Li, Synthesis, curing behavior and thermal properties of fluorine containing benzoxazines, *Eur. Polym. J.* 46 (2010) 1024–1031.
- [59] T. Fang, D.A. Shimp, Polycyanate esters: Science and applications, *Prog. Polym. Sci.* 20 (1995) 61–118.
- [60] S.J. Martin, J.P. Godschalx, M.E. Mills, E.O. Shaffer, P.H. Townsend, Development of a low-dielectric-constant polymer for the fabrication of integrated circuit interconnect, *Adv. Mater.* 12 (2000) 1769–1778.
- [61] M.F. Durstock, M.F. Rubner, Dielectric properties of polyelectrolyte multilayers, *Langmuir* 17 (2001) 7865–7872.